Electrophoretic Collision of a DNA Molecule with an Insulating Post

Greg C. Randall and Patrick S. Doyle

Department of Chemical Engineering, Massachusetts Institute of Technology, Cambridge, Massachusetts 02139, USA

(Received 16 January 2004; published 29 July 2004)

We study the dynamics of single DNA molecules driven by an electric field into a stationary obstacle. These collisions are broadly classified as "hook" and "roll-off" events. We show that obstacle-induced electric field gradients stretch impacting DNA and thus greatly influence the hooking probability. Consequently, in addition to collision geometry, determination of the hooking probability depends on the Deborah number (De) for $0.5 < \mathrm{De} < 40$. Individual DNA impact dynamics are highly configuration sensitive, characteristic of polymers in elongational flows and fields.

DOI: 10.1103/PhysRevLett.93.058102 PACS numbers: 87.14.Gg, 82.35.Rs, 83.50.–v, 87.15.–v

Polymer collisions occur in many settings, ranging from biological macromolecule interactions [1], to the rheology of polymer melts [2], to DNA electrophoresis [3]. Although typically ignored, obstacles in microfluidic devices can induce complex flows and fields that can complicate polymer-obstacle interactions. In the past ten years, the single polymer-obstacle collision problem has drawn increasing attention because the holdup time for a hairpin hooking collision depends on the length of the polymer and therefore serves as a possible way to size-separate polyelectrolytes such as DNA. Proof-of-principle separations with this mechanism have already been performed using a sparse array of obstacles [4,5]. Optimization and improvement of these devices require knowledge of the poorly understood microscale physics.

Hooking collisions were first observed experimentally in agarose gels [6] and later in dense microfabricated obstacle arrays [7,8]. Recently they have been observed in other obstacle-filled environments [4,5,9]. However, no experimental work has been done to systematically study the impact dynamics of single DNA-obstacle collision events. Single collisions have been addressed by simulations which have generally considered point-sized obstacles and the infinite electric field limit [10–13]. Recent improvements have been done to study moderate electric fields with small obstacles [14], and strong electric fields with finite-sized conducting obstacles [15]. However, most collision-based separation devices employ insulating obstacles on the order of the DNA size. Simulations and analysis of realistic insulating, finite-sized obstacles have not been considered.

When obstacles have a finite size, in addition to hooking collisions, "roll-offs" can occur where the DNA impacts the obstacle and simply advects around one side [15]. For example, Figs. 1(a) and 1(b) show our experimental images of λ-DNA (48.5 kbp) impacting an obstacle during both a roll-off and a hooking collision. The geometric parameters R_{obs}/R_g (ratio of the obstacle radius to the DNA equilibrium radius of gyration) and b/R_g (ratio of the offset between an impacting molecule's center of mass and the obstacle center to R_g [16]), are naturally important for determination of the hooking probability. As both R_{obs}/R_g and b/R_g increase, it becomes less likely for an impacting DNA configuration to span the obstacle, so more and more collisions are roll-offs [15]. However, little else is known of this important transition between roll-offs and hooking collisions.

In this Letter, we study the *impact dynamics* of an electrophoretically driven DNA molecule colliding into

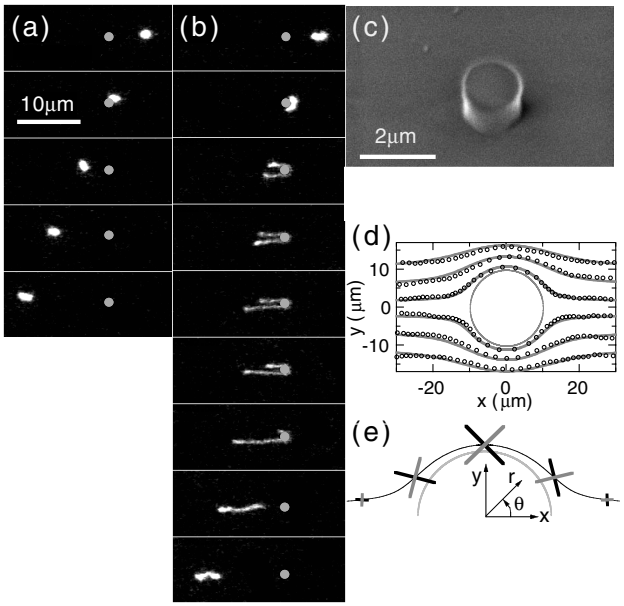

FIG. 1. Time-lapse images (0.17 s intervals) of (a) a roll-off collision and (b) a hooking collision of λ-DNA with an obstacle ($R_{\mathrm{obs}} = 0.8\ \mu$m) at $E = 15$ V/cm ($\mathrm{Pe} = 5.5$, $\mathrm{De} = 13$). Obstacles are artificially added for clarity. (c) scanning electron microscopy image of a typical PDMS obstacle with $R_{\mathrm{obs}} = 0.8\ \mu$m. (d) Electrophoretic traces of 0.5 μm diameter carboxylated beads at $E = 29$ V/cm around a PDMS obstacle ($R_{\mathrm{obs}} = 10\ \mu$m). Solid lines indicate expected 2D trajectories around an insulating cylinder in an unbounded conductor. (e) Primary axes of extension (black) and compression (gray) (with length normalized by $\dot{\epsilon}$) along a typical field line.

 0031-9007/04/93(5)/058102(4)$22.50

a single insulating obstacle in a microfluidic device. The DNA molecule is characterized by its persistence length a, contour length L, diffusivity D, relaxation time τ, and electrophoretic mobility μ [17]. The preimpact DNA molecule has an equilibrium configuration [18] in a uniform electric field with magnitude E far from the obstacle. We show that in addition to b/R_g and $R_{\rm obs}/R_g$, the hooking process is governed by a dynamic parameter $\mathrm{De} = 2\mu E\tau/R_{\rm obs}$, the ratio of the rate of maximum DNA deformation to DNA relaxation in an obstacle-induced field gradient. For reference, we also define the Peclet number $\mathrm{Pe} = \mu Ea/D$. Pe is used to properly scale the electric field when considering either the extension of an end-tethered chain or the collision of a DNA with a point obstacle in a *uniform* electric field [11,14].

We designed a model experimental system [19] to study single collisions of λ-DNA with stationary microfabricated PDMS [poly(dimethylsiloxane)] obstacles [Fig. 1(c)]. We stain λ-DNA with a fluorescent dye (TOTO-1, 4.7:1 bp:dye molecule), apply an electric field, and observe single DNA molecule dynamics using fluorescence videomicroscopy.

The electrical conductivity of a PDMS obstacle is $\sim$12 orders of magnitude smaller than that of the buffer, so these obstacles deflect electric current. This is generally true for many other materials used for obstacles in lab-on-chip processes, e.g., glass, plastics, colloids, or emulsion drops. Recently, others have explored applications using insulating obstacles such as size-excluded trajectory DNA separations [20] and dielectrophoretic focusing [21] (Note: dielectrophoretic forces are negligible in our study). However, here we will focus on how the obstacle-induced electric field gradients *deform* DNA molecules, which is intimately linked to hook formation.

To validate that the obstacles are insulating, we track electrophoretic motion of fluorescent beads around an obstacle [Fig. 1(d)]. We find that the obstacles are insulating and sufficiently isolated from wall effects since the field lines of our confined system match the solution for an isolated insulating cylinder (confirmed by finite element calculations). In our obstacle-centered coordinate system of Fig. 1(e), the electrophoretic velocity field $\mathbf{v}$, i.e., the velocity of a negatively charged object with mobility μ, near an obstacle is

$$\mathbf{v} = -\mu E\cos\theta\left(1 - \frac{R_{\rm obs}^2}{r^2}\right)\mathbf{e}_r + \mu E\sin\theta\left(1 + \frac{R_{\rm obs}^2}{r^2}\right)\mathbf{e}_\theta. \quad (1)$$

Note that this is a nonhomogeneous effective velocity field characterized by front and rear stagnation points. Analogous to hydrodynamic flow gradients deforming polymers, the electric field gradients induce deformation of a flexible, charged polymer like DNA. Because hook formation requires DNA configurations that span the obstacle during impact, we argue that velocity field gradients greatly affect the probability of forming a hooked configuration, $P_{\rm hook}$, on finite-sized obstacles. The characteristic length scale of these field gradients is $R_{\rm obs}$, thus we would expect them to affect $P_{\rm hook}$ when $R_{\rm obs}/R_g \gtrsim 1$. Before addressing this intermediate regime, it is useful to first look at the large obstacle limit ($R_{\rm obs}/R_g \gg 1$) where deformation must govern $P_{\rm hook}$.

To quantify the extension of a flexible polyelectrolyte in the velocity field of Eq. (1), we determine the velocity field gradient. It is predictably symmetric, characteristic of a potential field. In terms of kinematics, local deformation in this field is pure *elongation*. By diagonalization, we can extract the velocity field gradient eigenvalues ($\pm 2\mu E R_{\rm obs}^2/r^3$) and eigenvectors. The positive eigenvalue is the strain rate $\dot{\varepsilon}$, and its corresponding eigenvector is the primary axis of extension, which are both spatially inhomogeneous [Fig. 1(e)]. We define De using the largest strain rate $\dot{\varepsilon}(R_{\rm obs}) = 2\mu E/R_{\rm obs}$, so that $\mathrm{De} = 2\mu E\tau/R_{\rm obs}$. Note that during a collision, the actual radial-dependent strain rate is ramped to this maximum value, indicating the possibility of preimpact deformation. Theoretically, for $\mathrm{De} < 0.5$ the molecule's internal relaxation modes dominate the effect of the field gradient and minimal stretching occurs, whereas for $\mathrm{De} > 0.5$ the field dominates and the molecule will strongly stretch [22].

We validate that De correctly describes the action of the obstacle-induced electric field gradients on a DNA molecule by investigating the predicted critical coil-stretch transition at $\mathrm{De} = 0.5$. Figure 2 shows the longest extension $x_{\rm ex}$ [23] of a λ-DNA molecule as a function of time during centerline ($b = 0$) collisions with large obstacles. Comparing Fig. 2(a) with 2(b), we see that at subcritical De ($\mathrm{De} = 0.25$) no molecules stretch beyond typical equilibrium values, whereas at supercritical De ($\mathrm{De} = 1$)

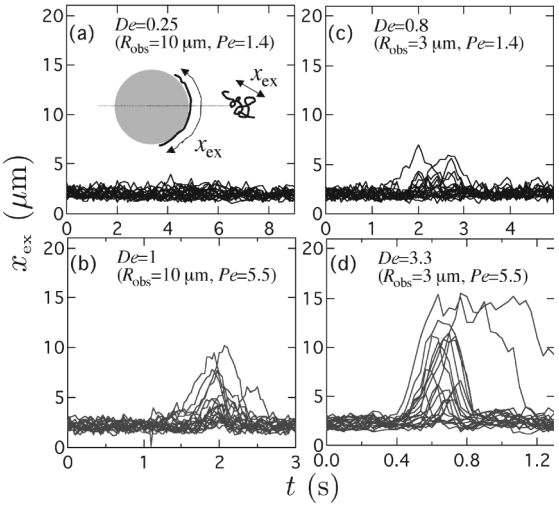

FIG. 2. Dynamic extension of centerline ($b = 0$) collisions with a large obstacle. $R_{\rm obs} = 10\ \mu$m [(a) and (b)], and 3 μm [(c) and (d)]. The contour length of the stained λ-DNA is 21 μm.

some do stretch. Keeping the two electric field strengths constant, thereby fixing Pe, we increase De by reducing the obstacle size from $R_{obs} = 10\ \mu$m to 3 μm. By comparing Fig. 2(a) with 2(c), i.e., passing from subcritical to supercritical De, we again observe the critical stretching transition. Similarly, Fig. 2(d) shows stronger stretching than the collisions of Fig. 2(b). Note that the only difference between these sets of experiments is the obstacle size. Previous collision studies [9] addressed only uniform field effects (e.g., unhooking time) governed by Pe. However, our results indicate that electric field gradients, characterized by De, govern the stretching of DNA molecules around large obstacles.

Each collision of Fig. 2 has the same impact parameter ($b = 0$), however the stretching behavior varies greatly from molecule to molecule. This is reminiscent of hydrodynamic elongational flow studies [24] which showed that the unraveling of a polymer in elongational flow is sensitive to its initial configuration. For the same accumulated strain (or residence time), initially open "dumbbell" configurations stretch faster than "kinked" and "folded" configurations. For comparison, we determine the accumulated strain experienced by each molecule by integrating the spatially dependent strain rate over the molecule's center-of mass trajectory. Figure 3 shows these results at De = 2 for large obstacles. The dark trajectories stop when any segment of DNA crosses $x = 0$. We include this cutoff because the primary axis of extension and its orthogonal primary axis of compression rotate along a given fieldline [Fig. 1(e)], causing compression of stretched DNA as it passes $x = 0$. We find that molecules which experience the same accumulated strain can exhibit vastly different stretching, e.g., ranging from $0.25L$ (slightly larger than an equilibrium coil) to $0.75L$ (strongly stretched) by a strain of 5. Microscopic observation of the coarse-grained preimpact configurations for each of these collisions shows that the strongly stretched molecules either exhibit some prestretching or initially have a "dumbbell" configuration aligned along the primary axis of extension. This is a strong indication that, as in elongational flows, the fate of an *individual* colliding DNA is highly sensitive to its preimpact configuration.

With this insight into large obstacle collisions, we now study P_{hook} with obstacles typical of current separation devices ($R_{obs}/R_g \sim 1$) [4,5]. We directly measure P_{hook} with our microchannel setup, defining a hooking collision as any collision in which the DNA molecule is simultaneously present in all four quadrants of our obstacle-centered coordinate system. Figure 4(a) shows the results of P_{hook} as a function of the impact parameter for collisions of λ-DNA into obstacles with $R_{obs} = 0.8\ \mu$m. For limiting behavior, we include simulation results of a point obstacle collision [25]. Note that the hooking probability is significantly lower than in the point obstacle limit ($R_{obs}/R_g \ll 1$) and increases as De increases. In the point obstacle limit, P_{hook} is *purely geometric*, dependent only on the DNA coil size. However, because P_{hook} increases with De, a dynamic effect underlies hook formation for finite-sized obstacles ($R_{obs}/R_g \gtrsim 1$), a result not predicted by any previous models. We claim that this amplification of hooking with De is a measurable effect of the deformation caused by obstacle-induced electric field gradients.

To probe the impact dynamics at large De, we employ a Brownian dynamics simulation technique [26,27]. Figure 4(b) shows P_{hook} as a function of b/R_g using a bead-spring chain (30 beads connected by wormlike springs [26]) and an insulating obstacle. As De increases above De $\sim$ 40, we observe saturation of P_{hook} below the point obstacle limit. At such strong strain rates, a coil affinely deforms into folded or kinked configurations whose average extension as a function of accumulated strain saturates and becomes independent of De for De $>$ 40 [28,29]. These electric field-driven collisions differ from homogeneous flows because De ramps up to its

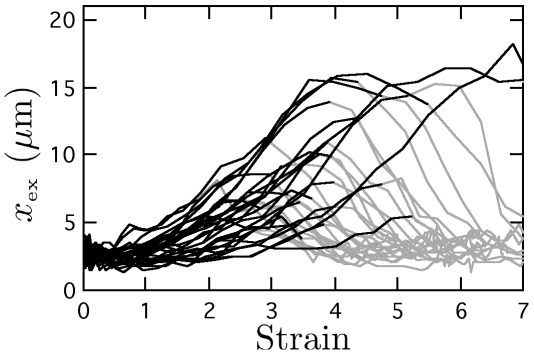

FIG. 3. Dynamic extension vs accumulated center-of-mass strain of 30 centerline ($b = 0$) collisions with a large obstacle ($R_{obs} = 10\ \mu$m) at De = 2 (dark lines). Compression on the backside of the obstacle is indicated by gray lines.

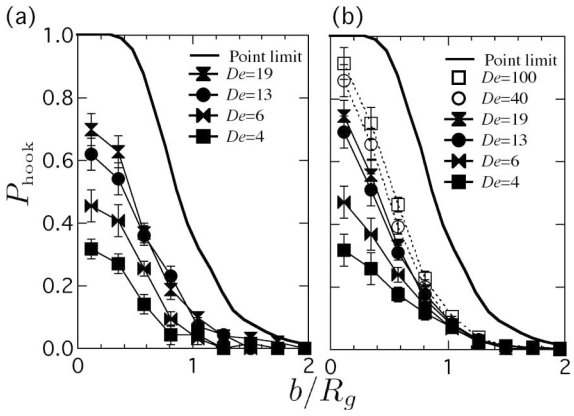

FIG. 4. (a) Experimental and (b) simulated hooking probability as a function of impact parameter. The obstacle radius is 0.8 μm ($R_{obs}/R_g = 1.1$). Statistics for each symbol are taken over an ensemble of 500 chains with a bin size of 0.23.

maximal value during the collision process, presumably reducing the importance of kinks and folds. However, the ramping is so steep ($\sim 1/r^3$) that it is nearly a step-function. Therefore, because elongation and hooking are intimately linked, we conclude that in the regime where $R_{\mathrm{obs}}/R_g \gtrsim 1$ and $0.5 < \mathrm{De} < 40$ we expect a *field-dependent* and *length-enhanced* hooking probability. By *length-enhanced* we mean that, for a given E and R_{obs}, larger molecules are more likely to form hooks not only due to their larger cross-section, but also due to field-gradient stretching effects (larger De).

In summary, this Letter clearly shows that obstacle-induced electric field gradients stretch DNA, so that in addition to two geometric parameters (R_{obs}/R_g and b/R_g), the hooking probability depends on a dynamic parameter (De). Furthermore, the electrophoretic velocity field near an insulating obstacle is purely elongational, which gives rise to *molecular individualism*, as seen in hydrodynamic flows.

This new insight into the physics of finite-sized obstacle collisions shows the necessity of including obstacle-induced field or flow gradient effects on flexible molecules in microdevices. The ability to stretch and compress DNA and other flexible molecules is crucial to the design of many current microfluidic processes. We have shown that obstacle induced electric field gradients act as a nonhomogeneous elongational field to stretch and compress DNA. For collision-based DNA separations, a field-dependent hooking probability is a measurable result of this generally ignored effect. Consequently, the field gradients introduce an additional length dependence to the separation scheme (De $\sim \tau$) and the DNA collision deformation is highly configuration sensitive. These ideas may be used to combat a major limitation in the usefulness of hooking collisions as a separation mechanism. In current separation obstacle courses [4], smaller DNA molecules may form more hooks overall than larger DNA because they relax back into coils more quickly after unhooking. This counteracts the tendency of larger DNA to lag behind the smaller DNA in the device due to longer collision times. A powerful application of this work would be to use obstacle induced field gradients to *force* compression of the chain after a collision. This has been observed in our experiments at the rear stagnation point of large obstacles [Fig. 3] and will be discussed elsewhere.

We thank Dr. K. Dorfman for stimulating discussions. This work was supported by a NSF CAREER Grant No. CTS-0239012.

[1] F. C. MacKintosh, J. Käs, and P. A. Janmey, Phys. Rev. Lett. **75**, 4425 (1995).
[2] G. Marrucci, J. Non-Newtonian Fluid Mech. **62**, 279 (1996).
[3] J.-L. Viovy, Rev. Mod. Phys. **72**, 813 (2000).
[4] P. S. Doyle, J. Bibette, A. Bancaud, and J.-L. Viovy, Science **295**, 2237 (2002).
[5] N. Minc *et al.*, Anal. Chem. **76**, 3770 (2004).
[6] L. Song and M. F. Maestre, J. Biomol. Struct. Dyn. **9**, 087 (1991).
[7] R. H. Austin and W. D. Volkmuth, Analusis **21**, 235 (1993).
[8] W. D. Volkmuth *et al.*, Phys. Rev. Lett. **72**, 2117 (1994).
[9] D. J. Olson *et al.*, Langmuir **17**, 7396 (2001).
[10] G. I. Nixon and G. W. Slater, Phys. Rev. E **50**, 5033 (1994).
[11] E. M. Sevick and D. R. M. Williams, Phys. Rev. E **50**, 3357(R) (1994).
[12] E. M. Sevick and D. R. M. Williams, Phys. Rev. Lett. **76**, 2595 (1996).
[13] P. André, D. Long, and A. Ajdari, Eur. Phys. J. B **4**, 307 (1998).
[14] P. D. Patel and E. S. G. Shaqfeh, J. Chem. Phys. **118**, 2941 (2003).
[15] P. M. Saville and E. M. Sevick, Macromolecules **32**, 892 (1999).
[16] Using the obstacle-centered coordinate system of Fig. 1(e), $b = |y_{\mathrm{DNA}} - y_{\mathrm{obs}}|$.
[17] We experimentally measure $D = 0.26\ \mu\mathrm{m}^2/\mathrm{s}$, $\tau = 0.19$ s, and $\mu = 1.7\ (\mu\mathrm{m\ cm})/(\mathrm{s\ V})$ in our microchannels and take $a = 53$ nm.
[18] Obstacles are spaced so that there is a minimum of 9 relaxation times (1.75 s) between collisions.
[19] We construct 2.5 cm-long, 50 μm-wide, and 2 μm-high PDMS microchannels by soft lithography [Y. Xia and G. Whitesides, Angew. Chem., Int. Ed. Engl. **37**, 550 (1998)]. Monodisperse λ-DNA were diluted in a buffer of 2.2X TBE, 3% β-mercaptoethanol, 0.07% PVP ($M_w = 10^6$, $c^* = 1.5\%$), and 0.07% ascorbic acid (viscosity = 1.3 cP). The additives were chosen to eliminate electro-osmotic flow and scavenge oxygen.
[20] L. R. Huang *et al.*, Phys. Rev. Lett. **89**, 178301 (2002).
[21] C.-F. Chou *et al.*, Biophys. J. **83**, 2170 (2002).
[22] R. G. Larson and J. J. Magda, Macromolecules **22**, 3004 (1989).
[23] When not on an obstacle, we represent the DNA molecule's 2D fluorescent image by an ellipse and x_{ex} is length of the major axis. When stretched on an obstacle, x_{ex} is the end-to-end arc length.
[24] T. T. Perkins, D. E. Smith, and S. Chu, Science **276**, 2016 (1997).
[25] We create ensembles of 500 bead-spring chains (30 beads connected by wormlike springs [26]) to model λ-DNA, and displace each chain's center-of-mass y coordinate to $+b$ (recall $y_{\mathrm{obs}} = 0$). If any bead in a chain has a y coordinate ≤ 0, then this configuration is considered a hook. Results agree with dynamic simulations of [12].
[26] P. S. Doyle, B. Ladoux, and J.-L. Viovy, Phys. Rev. Lett. **84**, 4769 (2000).
[27] P. T. Underhill and P. S. Doyle, J. Non-Newtonian Fluid Mech. (to be published).
[28] R. G. Larson, H. Hu, D. E. Smith, and S. Chu, J. Rheol. (N.Y.) **43**, 267 (1999).
[29] R. G. Larson, Rheol. Acta **29**, 371 (1990).